

Article

A GIS-Based Multidimensional Evaluation Method for Solar Energy Potential in Shanxi Province, China

Liang Cui *, Junrui Zhang, Yongyong Su and Siyuan Li

College of Resources and Environment, Shanxi University of Finance and Economics, Taiyuan 030006, China

* Correspondence: 20161026@sxufe.edu.cn; Tel.: +86-351-766149

Abstract: Solar energy is considered one of the most hopeful alternative sources to avoiding dependence on fossil fuels, and it does not cause any air pollution. GIS-based solar energy potential evaluation is mainly focused on regional scale; further, more solar energy potential evaluation with building scale is calculated through observation data and mathematical model. Therefore, in this paper, a GIS-based joint solar energy potential evaluation is developed to evaluate the distributed photovoltaic potential and centralized photovoltaic potential. Shanxi province in China, which has abundant coal resources, is used as the study area. The raster grid scale is used as the minimum research scale, which could not only deal with the distributed photovoltaic potential but could also calculate the centralized photovoltaic potential. The obtained results indicate that the developed method could effectively deal with problems associated with the distributed photovoltaic potential and centralized photovoltaic potential in the raster grid scale.

Keywords: solar energy; potential; GIS; MCDA; Shanxi province



Citation: Cui, L.; Zhang, J.; Su, Y.; Li, S. A GIS-Based Multidimensional Evaluation Method for Solar Energy Potential in Shanxi Province, China. *Energies* **2023**, *16*, 1305. <https://doi.org/10.3390/en16031305>

Academic Editors: Kittisak Jemsittiparsert and Thanaporn Sriyakul

Received: 29 December 2022

Revised: 17 January 2023

Accepted: 24 January 2023

Published: 26 January 2023



Copyright: © 2023 by the authors. Licensee MDPI, Basel, Switzerland. This article is an open access article distributed under the terms and conditions of the Creative Commons Attribution (CC BY) license (<https://creativecommons.org/licenses/by/4.0/>).

1. Introduction

Energy demand has increased since the industrial revolution. Well-known, burning fossil fuels, such as coal, natural gas and oil, generate air pollution and cause environmental pollution problems [1]. Due to the intensification of industrialization and the excessive use of fossil fuels, the demand for renewable energy is increasing. Solar energy is a kind of infinite, rich, green, free, reliable, sustainable and renewable energy [2]. Solar energy is considered one of the most hopeful alternative sources to avoiding dependence on fossil fuels and has great potential to meet the world's energy demand [3].

Consequently, a number of researchers have made efforts to develop effectual methods to evaluate the potential of solar energy with the background of dioxide carbon emission reduction. Remote sensing technology was used to assess solar energy, and the results showed a high spatial resolution and sufficient temporal resolution compared with ground station data [4]. The solar energy in the northern part of Ethiopia was estimated through the primary data; the results indicated that the potential of solar energy resources can be determined [5]. Escobar et al. (2014) presented a satellite estimation model to evaluate the energy resource in Chile; the results indicated that radiation levels are high throughout the country and that northern Chile has the highest solar energy resources in the world [6]. Xu et al. (2021) proposed a multidimensional evaluation method to calculate solar energy potential in Wuhan China with the block-scale, and they proposed the application strategies to optimize photovoltaic applications in different industrial blocks [7].

Estimation of solar energy potential must be specific to a particular administrative region, which involves various natural and social factors. Geographic Information Systems (GIS) is a useful tool to model the renewable energy over a region. Many researches focused on the application of Multi-Criteria Decision Analysis (MCDA) method in the solar energy potential assessment. For example, Rylatt et al. (2001) presented a solar energy programming system, which supported the decisions in photovoltaics, passive solar

gain and solar water heating [8]. Groppi et al. (2018) illustrated a GIS-based model for urban solar energy potential, and the result has found the most suitable solar potential exploitation area in the study region [9]. An Ordered Weighted Averaging (OWA) method was used to evaluate the solar energy potential and to determine the optimal installation areas of the solar power plants in Iran [10]. However, the GIS-based solar energy potential evaluation was mainly focused on regional scale or block-scale without considering a joint evaluation of urban building and rural areas.

The urban buildings' solar energy potential in block-scale is crucial to the sustainable development of the city. Previous studies were mainly focused on estimating the radiation of the building roofs or on drawing regional solar maps [11]. These regional solar maps were widely used to find out the potential of the solar photovoltaic industry, such as the solar maps of China, Canada, USA and Spain [12–16]. The main shortage is that research on block-scale is too detailed, and the regional scale is too rough.

Recently, the regional and global solar energy potential have been assessed by many researchers, both on the regional scale and on the roofs of buildings. However, most scholars only evaluate natural solar radiation, without considering feasibility and economy. Fillol et al. calculated the average daily global horizontal irradiation (GHI) by remote sensing to evaluate the solar energy potential in the Guiana Shield [17]. Huang et al. built a GIS-based solar photovoltaic potential assessment model to identify the suitable area for solar power stations' operation but failed analysis of the solar energy potential [18]. Moreover, potential building scale solar energy, especially roof solar energy, has been researched by the studies, and many methodologies have been explored [19]. Polo et al. used satellite data combined with solar radiation to evaluate the solar resources in Vietnam and to determine the solar potential for concentrating solar power [20]. Li et al. considered the resource, technology and economic potential and investigated the urban residential buildings' solar potential [21]. Zhang et al. analyzed the solar energy potential in China and estimated the solar energy potential from technology, geography and economy views [22].

GIS-based solar energy potential evaluation is mainly focused on regional scale; further, more solar energy potential evaluation with building scale is calculated through observation data and mathematical model. Therefore, in this paper, a GIS-based solar energy potential multi-criteria decision analysis model (GIS-MCDA) is developed to evaluate the distributed photovoltaic potential and centralized photovoltaic potential in the raster grid scale. Shanxi province in China, which has abundant coal resources, is used as the study area. Meanwhile, the region is facing the problem of fossil energy transformation. The raster grid scale is used as the minimum research scale, which could not only deal with the distributed photovoltaic potential but could also calculate the centralized photovoltaic potential. The obtained results will be useful for the local government to improve the local energy structure.

This paper is organized as follows: First, the spatial distribution and changing trend of solar energy resources in Shanxi province are researched. Then the spatial distribution of a suitable area of solar energy resources in Shanxi is calculated. At last, the potential of solar energy in Shanxi is presented.

The development of solar energy is constrained by topography, land use types, technical conditions and land use policies. In this study, solar resource endowment, slope, aspect, land use and population density are considered evaluation indices.

2. Data Source and Research Method

2.1. Study Area and Data Source

Shanxi province is situated on the east side of the Loess Plateau, China. It is a plateau between the valleys of the middle reach of Yellow River and the Taihang Mountains. The topography of Shanxi province is low in the southwest and high in the northeast. In the east is the Zhongshan Plateau with Taihang Mountain as the main vein and Qinlu Plateau as the main body. The middle part is a multi-font beaded basin. The west side is the Lvliang Mountain as the main body of the mountains and the Yellow River east bank loess as continuous coverage of the Loess plateau [17]. The interior of the province is undulating.

Landforms are complex and diverse, mainly mountainous and hilly, while plains and valleys account for a relatively small area, as shown in Figure 1.

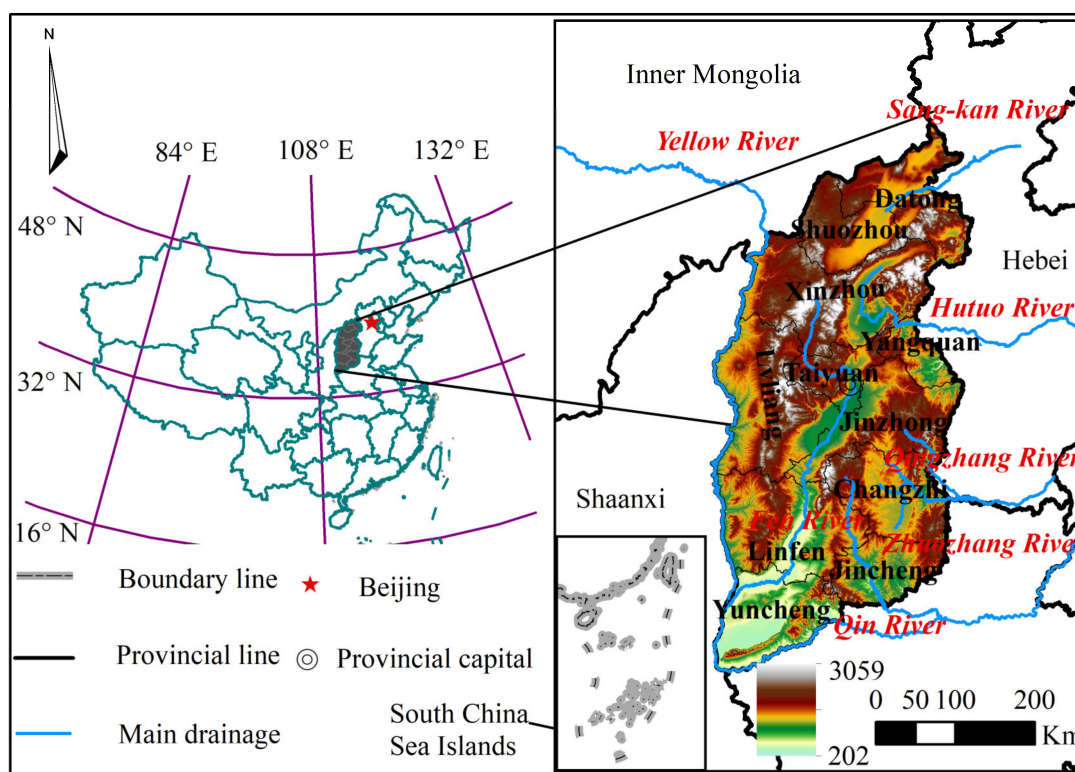


Figure 1. Schematic map of the study area.

By 2020, the installed capacity of grid-connected wind power in Shanxi province was 19.74 million kW, and the annual accumulative power generation was 26.57 billion kWh. The installed capacity of grid-connected solar power was 13.087 million kW, and the total annual photovoltaic power generation was 15.86 billion kWh. Their combined installed capacity accounts for 31.6% of the province's installed power generation capacity and 12.5% of its generating capacity. In 2021, Shanxi government issued the "Shanxi 14th Five-year Plan and 2035 Vision Target Outline", which points out that vigorously developed clean energy promotes the coordinated and orderly development of new energy growth, consumption and energy storage, promotes the complementary development of various energy sources and forms a green and diversified energy supply system [23].

The meteorological data used in this research were downloaded from the Daily Data Set of China Surface Climatic Data from 1987 to 2016 (<http://data.cma.cn/>; accessed on 10 June 2021). The meteorological data covered daily total horizontal solar radiation and daily sunshine hours (Figure 2). The land use data in 2020 were obtained from Landsat8 remote sensing image data updated by the Data Center for Resources and Environmental Sciences, Chinese Academy of Sciences (<http://www.resdc.cn>; accessed on 5 June 2021). The remote sensing data of the research was based on Landsat 8 OLI in 2020. DEM data were downloaded from geospatial data cloud platform with a resolution of 90 m × 90 m (<http://www.gscloud.cn/>; accessed on 3 July 2021). The administrative vector data used in the paper come from national basic geographic information data in the National Geographic Information Resource Catalogue Service system (<https://www.webmap.cn/>; accessed on 7 September 2021), and the data are based on the 2000 National geodetic coordinate system. Social and economic data, such as electricity consumption of the whole society and resident population data of Shanxi province and its cities, are all from the Shanxi Statistical Yearbook and Statistical bulletin for national economic and social development [24–26].

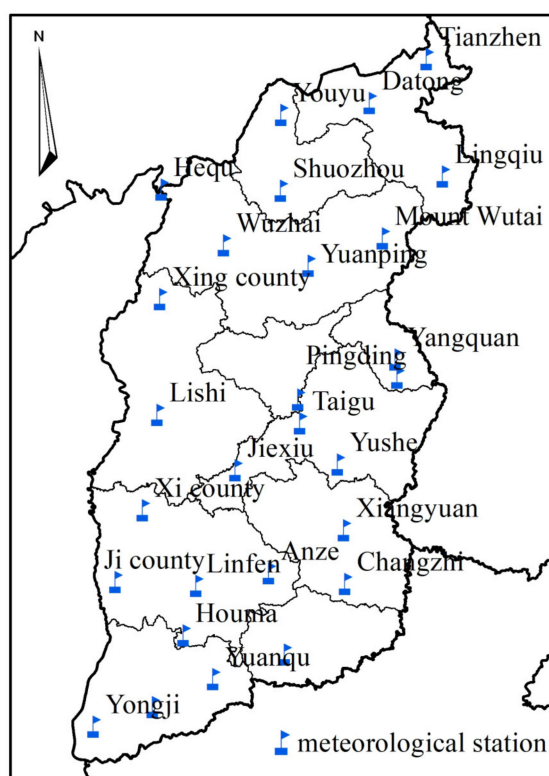


Figure 2. Study area and meteorological stations.

2.2. Climatological Calculation Method of Total Solar Radiation in Horizontal Plane

The amount of solar radiation arriving on the earth's surface is the basis of solar resource assessment and resource utilization potential accounting. However, there are only three meteorological stations with radiation observation records in Shanxi province, namely Datong, Taiyuan and Houma meteorological stations, with limited data that cannot meet the needs of refined solar resource assessment. Therefore, in order to carry out refined assessment of regional solar energy resources and analysis of development and utilization prospects, it is necessary to achieve indirect acquisition of total solar radiation in horizontal planes of stations or regions without radiation observation data through relevant calculation methods or satellite remote sensing data.

The solar total radiation calculation model is used to calculate the horizontal solar total radiation climatology. The model calculates the solar radiation received by the ground by building the relationship between the sunshine hours and the total horizontal solar radiation. The calculation formula is as follows [27]:

$$R_s = R_a \cdot \left(a + b \frac{H}{H_0} \right) \quad (1)$$

where R_s and R_a are the total solar radiation on the lunar horizontal plane and the solar radiation outside the moon (astronomical radiation), respectively (MJ/m^2). a and b are, respectively, empirical coefficients calculated based on measured radiation data; H and H_0 are monthly sunshine hours and monthly possible sunshine duration, respectively. Its ratio represents the percentage of sunlight per month, s .

The monthly extraneous solar radiation, R_a , could be obtained by summing the monthly extraneous solar radiation daily:

$$R_d = \frac{24 \cdot 3600}{\pi} - EDNI \cdot \left[\cos \phi \cos \delta \sin \omega_s + \frac{\pi \omega_s}{180} \sin \phi \sin \delta \right] - 10^6 \quad (2)$$

$$EDNI = E_0 \left(1 + 0.033 \cos \frac{360n}{365} \right) \quad (3)$$

$$\delta = 23.45 \cdot \sin \left(360 \cdot \frac{284 + n}{365} \right) \quad (4)$$

$$\omega_s = \arccos(-\tan \phi \tan \delta) \quad (5)$$

$$H_0 = \frac{24}{\pi} \omega_s \quad (6)$$

In the above formula, $EDNI$ stands for extraterrestrial normal solar irradiance (W/m^2). E_0 is the solar constant, take $1366.1 W/m^2$ with the range 368–2016. ϕ is latitude, $90^\circ \leq \phi \leq 90^\circ$. δ stands for solar declination, with the range $-23.45 \leq \delta \leq 23.45$. ω_s is the hour angle at sunset. μ stands for product day which means the ordinal number of the date in a year, with value ranges from 1–365/366.

The empirical coefficients a and b are determined by the least squares linear regression of R_s/R_a to H/H_0 . The calculation formula is as follows [28]:

$$\begin{cases} b = \frac{\sum_{i=1}^n (s_i - \bar{s})(y_i - \bar{y})}{\sum_{i=1}^n (s_i - \bar{s})^2} \bar{s} \\ a = \bar{y} - b \cdot \bar{s} \end{cases} \quad (7)$$

where s_i is the percentage of sunshine per month year by year. \bar{s} is the mean monthly sunshine percentage per year. y_i is the annual ratio of the monthly amount of horizontal radiation to the monthly amount of extraterrestrial solar radiation. \bar{y} represents the average value of the ratio of the monthly total horizontal radiation amount to the monthly solar radiation amount outside the earth in past years. n is the number of samples.

The calculation method of the total solar radiation in horizontal plane of the station without radiation observation data is as follows. Firstly, according to the data of total horizontal solar radiation, lunar extraterrestrial solar radiation and monthly sunshine from 1987 to 2016 at 21 radiation observation stations in Shanxi and surrounding provinces, coefficients a and b are obtained by using the least square method; secondly, Kriging interpolation method is used to interpolate coefficients a and b in the previous step to obtain the coefficients a and b of 25 meteorological stations in Shanxi province; finally, the annual monthly radiation data of each station from 1987 to 2016 is estimated through Equation (1).

2.3. Kriging Interpolation

Kriging interpolation is used in spatial data processing. The calculation method is as follows [29]:

$$z_0 = \sum_{i=1}^S z_x \cdot W_x \quad (8)$$

In the above formula, Z_0 is to be valued; S is the number of known points; Z_x is what we know at point x ; and W_x is the weighting coefficient of point x . It can be solved by a set of simultaneous equations. As shown below [29]:

$$\begin{cases} \sum_{i=1}^n \lambda_i = 1 \\ \sum_{i=1}^S \lambda_i Cov(x_i, x_j) - \beta = Cov(x_i, x_j) \end{cases} \quad (9)$$

where, $Cov(x_i, x_j)$ is the covariance between these two points; β is the Lagrange multiplier; and $Cov(x_i, x_j)$ is the covariance between the predicted value and the known value at point x .

The semi-variogram models commonly used in Kriging algorithm mainly include Gaussian model, linear model, spherical model and exponential model. When interpolating

meteorological element field, spherical simulation has better interpolation effect, which not only considers the randomness of reservoir parameters but also considers the correlation of reservoir parameters. Under the condition of the minimum interpolation variance, the optimal linear unbiased interpolation is given, and the interpolation variance is also given. The expression of the spherical model is presented as follows [29]:

$$\gamma(h) = \begin{cases} 0 & h = 0 \\ C_0 + C\left(\frac{3h}{2a} - \frac{h^3}{2a^3}\right) & 0 < h \leq a \\ C_0 + C & h > a \end{cases} \quad (10)$$

where $\gamma(h)$ is the spatial variation function; C_0 is the Nugget value that means the semi-variation when the sample pair distance is 0 represents the measurement and analysis error or small difference; C is the structural variance that represents variation due to non-random causes; $C_0 + C$ represents the base value that represents the maximum variation of the variable; h is the step length; and a is variation.

2.4. Solar Energy Resource Assessment Methods

The assessment of regional solar energy resources includes two aspects. The first aspect is the evaluation of the inherent solar resource endowment conditions of the region. Based on the four indicators of solar resource abundance, total horizontal radiation stability, available days of solar resources and sunshine stability, this study completed the assessment of the solar resource endowment conditions of Shanxi province. The level of solar energy resource abundance reflects the solar energy resource endowment of a region. The stability of horizontal total radiation and sunshine reflects the magnitude and state of the annual change of solar energy resources in a region. The number of days available for solar energy reflects whether the solar energy resources in a day are available.

The second aspect of the assessment is the calculation of the photovoltaic power generation potential of solar energy resources in Shanxi province at the emerging stage, according to the solar energy spatial distribution evaluation results in Shanxi province. In this study, the single crystal silicon photovoltaic cell module JNMM60 is selected as the reference module to calculate the solar photovoltaic power potential. The cell module is produced by local company JINENERGY which is mostly used in Shanxi province. The cell has high efficiency, and the output power of JNMM60 is 91.2% in 10 years and 80.7% in 25 years. The relevant parameters of MNMM60 are shown in Table 1.

Table 1. Parameters of JNMM60 photovoltaic module.

Component Type	Peak Power/W _p	Component Size/mm	Component Area/m ²	Photoelectric Conversion Efficiency/%
JNMM60	320	1665 × 996 × 35	1.66	19.3

The study takes the above type of photovoltaic module as reference to calculate the potential of solar photovoltaic power generation in the region. The calculation formula is shown below:

$$E_p = D_T \cdot \frac{P_{AZ}}{E_S} \cdot K \quad (11)$$

E_p is annual theoretical energy generation; D_T represents annual peak sunshine hours (h/a) (refer to the general peak sunshine hours of cities in Shanxi province in recent years); P_{AZ} represents the installed capacity of components (kWp); E_S represents irradiance under standard conditions (it is a constant (1 kW·h/m²)); K represents the combined efficiency coefficient, according to relevant studies, the efficiency coefficient is usually 75~85%, and the comprehensive efficiency coefficient is uniformly taken as 80% in the research [30].

The installed capacity of the modules is the sum of the nominal power of the photovoltaic modules, and the calculation formula is as follows:

$$P_{AZ} = W_p = \frac{W_a}{A} \cdot W_m \quad (12)$$

where W_p represents the peak total power of photovoltaic modules; W_a represents the area of photovoltaic modules that can be installed; and A represents the area occupied by photovoltaic modules per unit. Considering the shading and other conditions, it is generally 3 times the area of the unit photovoltaic module, $A = 5 \text{ m}^2$. W_m is the peak power of the photovoltaic modules adopted, $W_m = 320 \text{ Wp}$.

3. Research Results

3.1. Spatial Distribution and Changing Trend of Solar Energy Resources in Shanxi Province

The spatial distribution of the 30-year climate average value of the total horizontal solar radiation of each meteorological station was interpolated by the Kriging interpolation method, and the results are shown in Figure 3.

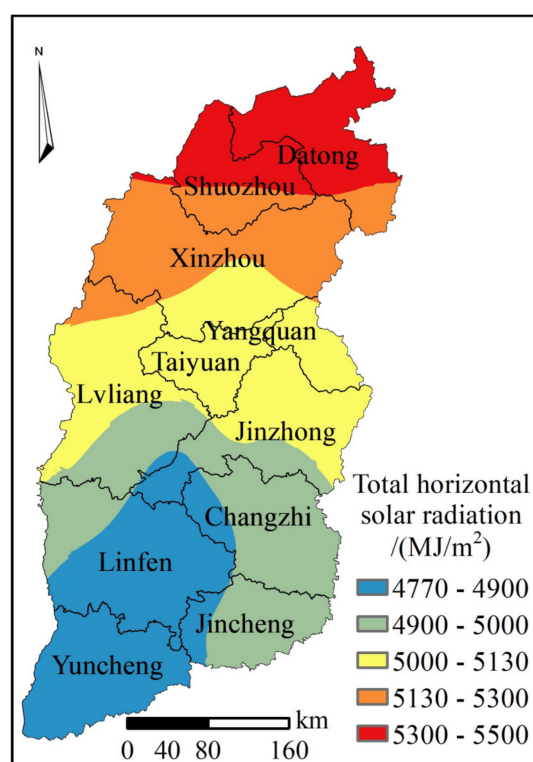


Figure 3. Spatial distribution of annual total horizontal solar radiation in Shanxi province.

The annual total horizontal solar radiation in Shanxi province gradually decreases from north to south, with significant difference between north and south, and the total horizontal solar radiation in the central basin area is smaller than that in the two sides of the same latitude, as shown in Figure 3. The high value region appeared in the northern part of Shanxi province, including Datong city and Shuozhou city, as well as the northeastern and northwestern parts of Xinzhou city. The lowest values are concentrated in the southwest of Shanxi province, especially in the Linfen Basin and the Yuncheng Basin. According to the regional statistics of the total horizontal solar radiation in Shanxi province, the annual average horizontal solar radiation of Shanxi province is 5090.89 MJ/m^2 . Datong city has the largest annual total horizontal solar radiation, reaching 5456.1 MJ/m^2 . Yuncheng city has the smallest annual total horizontal solar radiation with an average annual horizontal solar radiation of only 4769.6 MJ/m^2 .

Figure 4 shows the spatial distribution of total horizontal solar radiation in spring, summer, autumn and winter in Shanxi province. The fluctuation range of total horizontal solar radiation in Shanxi province varies from 160 MJ/m^2 to 300 MJ/m^2 . Among the four seasons, the total horizontal solar radiation is the largest in summer, and the difference between regions is also large. In winter, on the contrary, the total horizontal solar radiation is lower in the four seasons, and the difference between different regions is small.

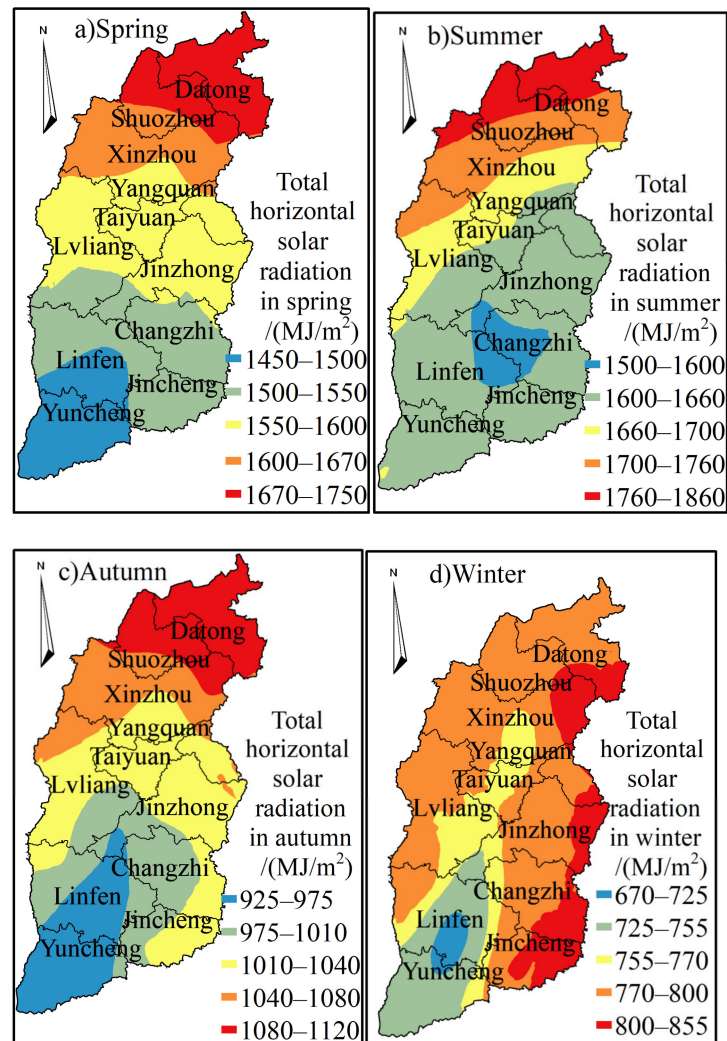


Figure 4. Spatial distribution of total horizontal solar radiation in Shanxi province.

In spring, the total horizontal solar radiation is between 1450 MJ/m^2 and 1750 MJ/m^2 , and the average total horizontal solar radiation of the province is 1576.43 MJ/m^2 , which shows an increasing trend from southwest to northeast. In the south of the province, the radiation value of the central basin is lower than that of the two sides of the same latitude, while in the Taiyuan Basin, the total solar radiation of the horizontal plane is relatively higher than that of other areas at the same latitude. In spring, the maximum horizontal solar radiation of 1750 MJ/m^2 appeared in the northern Datong city and Shuozhou City, while the minimum value appeared in the central part of Yuncheng City.

In summer, the total horizontal solar radiation is higher than 1500 MJ/m^2 , and the average total horizontal solar radiation is 1670.16 MJ/m^2 . The solar energy resources are the best in the four seasons at the same time the regional difference is also the largest; the regional fluctuation is 360 MJ/m^2 . The maximum value is 1860 MJ/m^2 in the northwest of Datong and Shuozhou.

In autumn, the total horizontal solar radiation of the whole province ranges from 925 MJ/m² to 1120 MJ/m², and the average regional radiation is 1022.89 MJ/m². The minimum value appears in Linfen Basin, and the total horizontal solar radiation of the whole province increases gradually in an elliptic shape from the center.

In winter, the total horizontal solar radiation in all regions of the province is the minimum difference in four seasons. The total horizontal solar radiation in all regions of the province is less than 900 MJ/m², and its spatial distribution is generally low in the central basin and high in the mountains on both sides. The maximum value is in the Wutai Mountain area, and the minimum value is in the Linfen Basin.

Table 2 shows the annual average sunshine hours of each meteorological station in Shanxi province. As shown in the table, Youyu meteorological station has the largest annual sunshine hours, which are 2823.74 h. Houma meteorological station has the lowest annual sunshine hours, which are 2049.23 h. Among all meteorological stations in the province, the annual sunshine hours of most meteorological stations are the maximum in spring and the minimum in winter.

Table 2. Annual average sunshine hours of each meteorological station in Shanxi province.

Meteorological Station Name	Sunshine Hours/h				
	Throughout the Year	Spring	Summer	Autumn	Winter
Tianzhen	2748.34	765.56	748.57	646.61	587.80
Datong	2655.68	744.96	739.68	627.25	543.79
Youyu	2823.74	787.89	767.01	667.27	601.57
Lingqiu	2564.95	736.78	657.92	606.13	564.12
Hequ	2490.28	711.56	725.28	585.50	467.95
Shuozhou	2515.00	705.82	671.18	602.55	535.45
Wutai	2685.13	758.09	639.23	645.69	642.12
Wuzhai	2563.29	711.18	693.13	608.43	550.54
Yuanping	2290.22	676.24	627.17	535.26	451.55
Linjin	2468.54	688.60	678.15	586.25	515.54
Pingding	2594.19	742.34	680.72	612.30	558.84
Taiyuan	2438.61	702.4	680.12	565.85	490.60
Lishi	2387.46	669.6	658.18	561.24	498.45
Taigu	2539.15	729.53	697.57	580.81	531.24
Yangquan	2401.89	690.07	605.21	572.05	534.56
Yushe	2339.96	660.46	606.07	549.6	523.83
Jiexiu	2108.52	642.41	545.89	473.29	446.94
Xi county	2492.28	690.81	674.62	576.63	550.22
Xiangyuan	2337.92	679.14	621.09	530.53	507.16
Anze	2187.66	629.67	581.98	497.42	478.59
Ji county	2261.82	636.03	608.77	517.50	499.53
Changzhi	2409.23	689.54	637.71	551.52	530.45
Linfen	2059.20	618.21	616.01	453.82	371.16
Houma	2049.23	612.70	601.28	439.40	395.85
Yangcheng	2413.39	684.52	653.59	545.16	530.13
Yuanqu	2050.42	585.38	543.70	467.82	453.53
Yuncheng	2093.62	600.96	636.34	448.26	408.07
Yongji	2146.00	608.07	659.75	462.14	416.04

The annual average sunshine hours of meteorological stations in Shanxi province were interpolated by the Kriging interpolation method, and the result is shown in Figure 5. The spatial distribution of annual average sunshine hours in the province is consistent with that of the total horizontal solar radiation in the province. Centered on Linfen Basin and Yuncheng Basin, it gradually increases from southwest to northeast and is lower in the south and higher in the north. The difference of annual average sunshine hours is obvious, and the difference between the maximum sunshine hours and the minimum sunshine hours is 800 h. The annual sunshine hours in the northwest of Shuozhou city and east of Datong city are above 2800 h, which is the largest in the province. Yuncheng city has the lowest annual average sunshine hours, which are 2113.57 h.

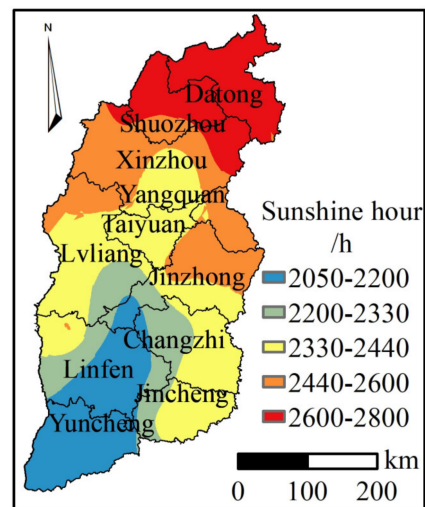


Figure 5. Spatial distribution of annual sunshine hours in Shanxi province.

The total horizontal solar radiation and annual sunshine hours of 28 meteorological stations in Shanxi province are statistically zoned by GIS (Figure 6). During 1987–2016 the total horizontal solar radiation and annual sunshine hours decreased at a rate of $74.94 \text{ MJ}/(\text{m}^2 \cdot 10\text{a})$ and $88.75 \text{ h}/10\text{a}$, respectively, and the decrease trend was significant ($p < 0.01$).

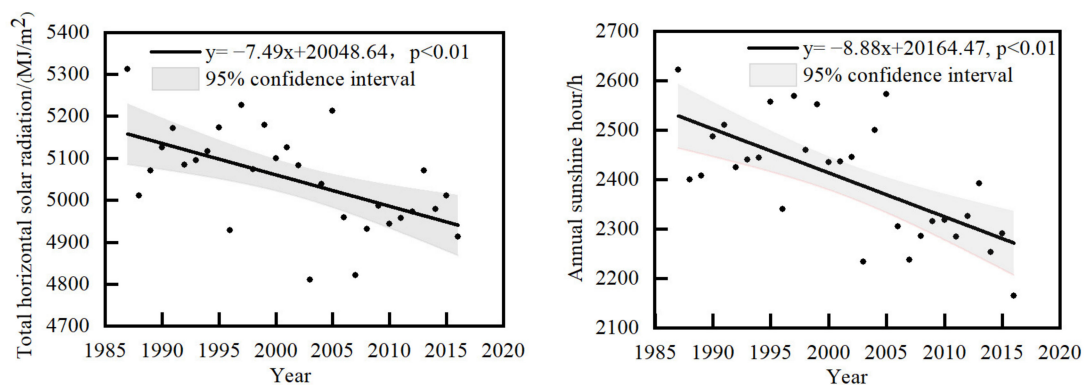


Figure 6. The variation trend of total horizontal solar radiation and annual sunshine hours in Shanxi province.

Figure 7 shows the spatial distribution of total horizontal solar radiation and annual sunshine hours of 28 selected meteorological stations in Shanxi province. As shown in the figure, only Datong and Taiyuan meteorological stations showed a significant increase in total horizontal solar radiation, while the other stations showed a decreasing trend. In terms of annual sunshine hours, only Datong, Taiyuan, Taigu and Yuanqu, four meteorological stations, showed an insignificant increase trend, while the other stations showed a decrease trend.

The abundance of solar energy resources is mainly measured by the total horizontal solar radiation. According to the index of middle-age horizontal solar radiation level in Table 3, the solar energy resources in Shanxi province are evaluated.

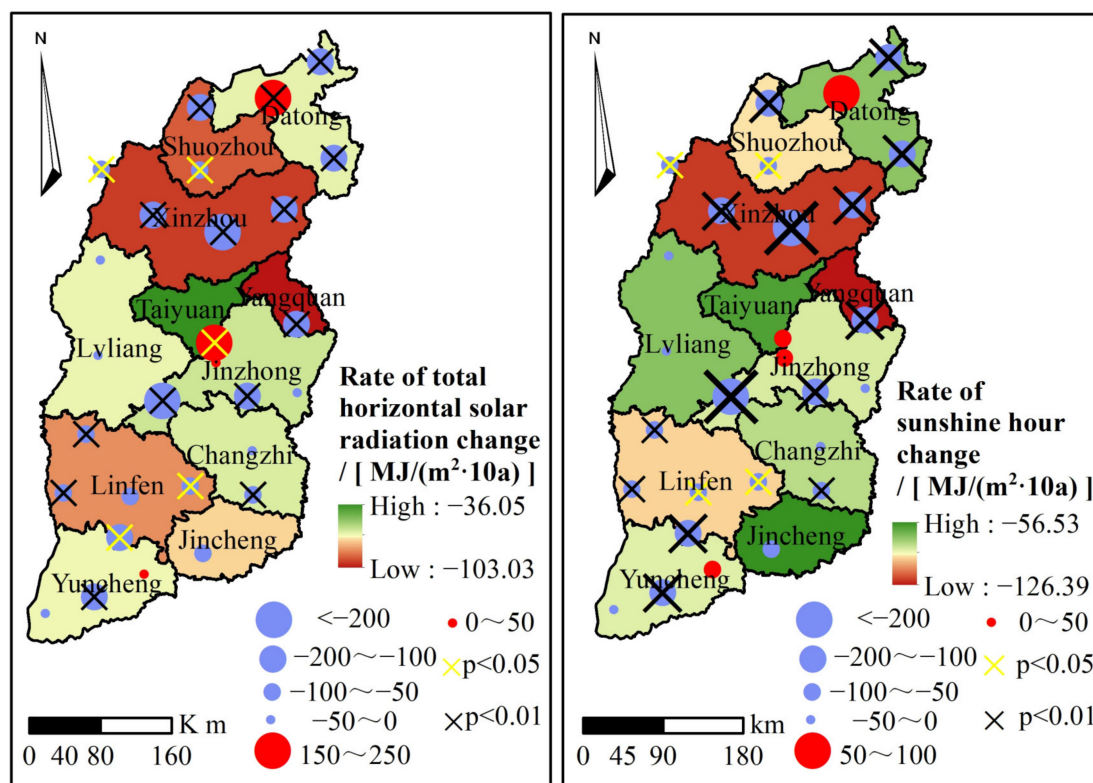


Figure 7. Spatial distribution of total horizontal solar radiation and annual sunshine hours in Shanxi province.

Table 3. Level of total horizontal solar radiation.

Level Symbol	Level Name	Graded Threshold/(MJ/m ²)
A	Most abundant	≥6300
B	Very rich	5040~6300
C	Abundant	3780~5040
D	General	<3780

The annual total horizontal solar radiation of Shanxi province is 4769.58~5443.57 MJ/m², and the average total horizontal solar radiation is 5049.32 MJ/m². In terms of specific cities, Datong, Shuozhou, Xinzhou, Taiyuan and Yangquan belong to the very rich region, while the rest belong to the abundant level (Figure 8).

3.2. Spatial Distribution of Suitable Area of Solar Energy Resources

The development of solar energy is constrained by topography, land use types, technical conditions and land use policies. In this study, solar resource endowment, slope, aspect, land use and population density are considered as evaluation indices. Based on GIS spatial analysis, each evaluation index is classified and quantified. Thus, the grid spatial distribution of suitable solar energy resources in Shanxi province is obtained. Evaluation index grading and evaluation rules are shown in Tables 4 and 5.

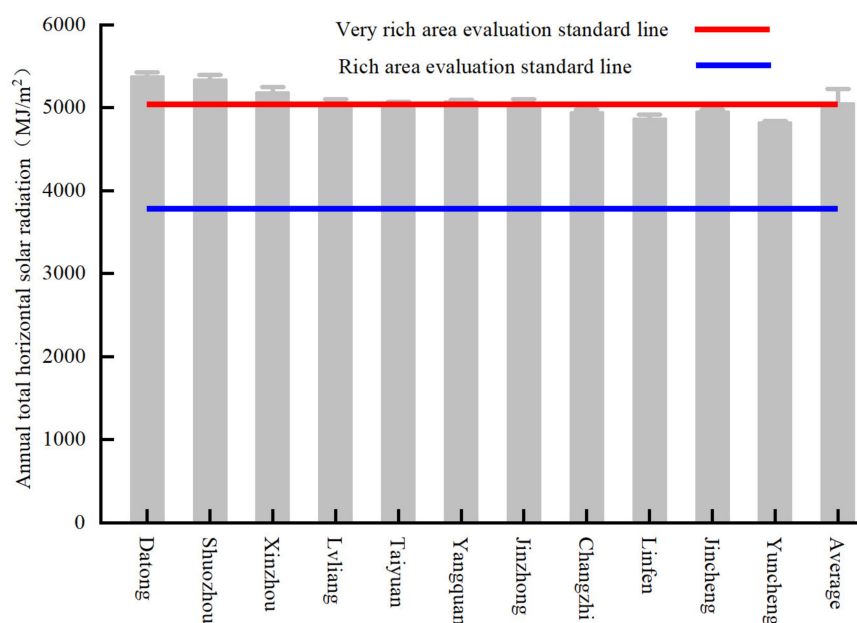


Figure 8. Solar energy resource abundance of cities in Shanxi province.

Table 4. Classification of suitable areas for solar energy resources in Shanxi province.

Evaluation Index	I	II	III	IV
Total horizontal solar radiation/MJ·m ⁻²	5200~5444	5000~5200	4900~5000	4769~4900
Total horizontal solar radiation stability	0.40~0.41	0.37~0.40	0.34~0.37	0.32~0.34
Available days/d	250~275	220~250	200~220	0~200
Sunshine hour stability	1~2	2~2.5	2.5~3	3~4
Slope/°	0~8	8~15	15~25	25~90
Aspect/°	-1/135~225	90~135/225~270	45~90/270~315	0~45/315~360

Table 5. Evaluation rules of suitable area for solar energy resource development in Shanxi province.

Assumption	Conclusions
(1) The land use types are cultivated land, forest land and water area; (2) Any area with a terrain slope greater than 25°.	Unsuitable zone
(1) The annual horizontal radiation is more than 5040 MJ/m ² , the slope is 0~15°, the slope direction is flat slope or south direction, and the land use type is low coverage grassland; (2) All unused land satisfying the terrain slope restriction conditions; (3) Urban, industrial, mining and rural residential land with a population density of 200 people/km ² .	The most suitable zone

Figure 9 shows the spatial distribution of suitable areas for the development of solar energy resources in Shanxi province. Among them, the area of unsuitable area is the largest, 103,563 km², accounting for 66.09% of the total area of Shanxi province. The general suitable area and more suitable area are 20,007 km² and 17,775 km², respectively. The most suitable area for the development of solar energy resources in Shanxi province is 15,201 km². The

development of solar energy resources are greatly restricted by the type of land use; as a result, the occupation of cultivated land, forest land and water area should be avoided as far as possible. Therefore, the regions with large areas unsuitable for development are mainly located in the regions with large areas of cultivated land and forest land in the province.

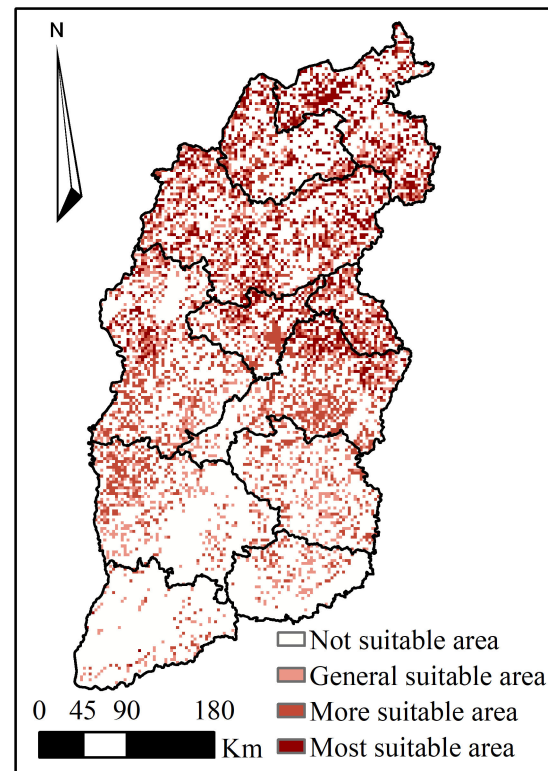


Figure 9. Suitable area of solar energy resource in Shanxi province.

3.3. Solar Energy Potential of Shanxi Province

The calculation of distributed solar photovoltaic potential in this paper is mainly aimed at roof distributed photovoltaic. By estimating the roof area of photovoltaic modules that can be installed in the province, the distributed solar photovoltaic potential can be quantified. The estimation of roof area is based on the scale of urban and rural construction land, including rural residential land, urban land and other construction land. The land use type is shown in Figure 10a. The area of the roof for distributed photovoltaic installation is estimated by the following formula:

$$W_a = \alpha \cdot S \cdot \beta \cdot k \quad (13)$$

In the formula, W_a is the roof area where photovoltaic modules can be installed, and α represents the penetration rate of photovoltaic cells. The ratio of the roof area that can be installed with photovoltaic modules to the total roof area is set at 25% in this study [31]. S is the area of urban land, industrial land and residential land; β is the building density of the house, which refers to the ratio of the building area to the land use area; and k is the proportion of the roof area to the floor area of the house, which is generally 60% [31].

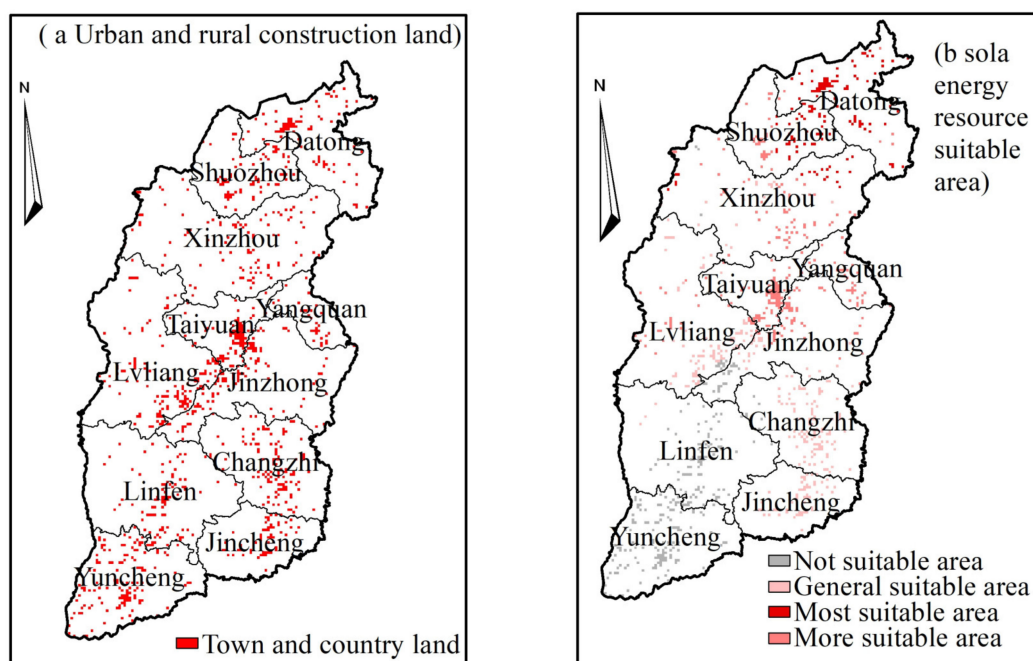


Figure 10. Urban and rural construction land and solar energy resource suitable area in Shanxi province.

As can be seen from Figure 10b, the development of urban and rural land solar energy resource in the province is mainly centered on the more suitable area. The most suitable area is mainly centered on the north of Shanxi province, including Datong, the east of Shuozhou and the northeast of Xinzhou. The more suitable area is mainly in Taiyuan, Yangquan and a small part of Jinzhong and Lvliang. The general suitable area is mainly concentrated in the southeast of Shanxi province, including Changzhi and Jincheng. The unsuitable area is mainly concentrated in Yuncheng, Linfen, southwest Jinzhong and a small part of southeast Lvliang.

The results of regional statistical processing show that the most suitable area of distributed photovoltaic development in Shanxi province is 1260 km². The more suitable area, general suitable area and unsuitable area are 2646 km² and 2547 km², respectively. According to Formula (11), the total annual potential of solar photovoltaic power generation in the most suitable area, more suitable area and general area is 11,218.26 GWh, 23,173.66 GWh and 21,785.75 GWh, respectively. The total annual power generation potential in the suitable area amounts to 56,177.68 GWh.

The GIS spatial analysis tool is used to calculate the distributed photovoltaic suitable area of each city and to calculate the annual power generation potential. The results are shown in Table 6. It can be seen that the annual power generation of Luliang is 8900.37 GWh, which has the largest area of urban and rural construction land. Linfen has a smaller area of urban and rural construction land; the annual power generation is 229.41 GWh. Yuncheng is not suitable for distributed photovoltaic development.

Based on the results of distributed photovoltaic development, the location suitable for centralized photovoltaic development in Shanxi Province is obtained on the basis of excluding distributed photovoltaic unsuitable area. Then the potential of centralized photovoltaic development in Shanxi province is calculated. In this study, the calculation of the potential of centralized photovoltaic power generation is only for the area where solar energy resources are developed and utilized in the most suitable area. Based on actual project experience, the photovoltaic installation capacity per unit area is set as 45 MW/km².

Table 6. Statistics of distributed photovoltaic installed capacity and annual power generation potential in suitable areas of Shanxi province.

City Name	Urban and Rural Construction Land (km ²)	Area for Installing Photovoltaic Modules/(km ²)	Installed Capacity (MW)	Peak Annual Sunshine Hours (h)	Annual Power Generation (GWh)
Datong	738	77.49	4959.36	1664.4	6603.49
Shuozhou	666	69.93	4475.52	1657.1	5933.11
Xinzhou	891	91.67	5866.56	1624.25	7623.01
Lvliang	1107	106.79	6834.24	1627.9	8900.37
Taiyuan	711	74.66	4777.92	1627.9	6222.38
Yangquan	270	28.35	1814.40	1609.65	2336.44
Jinzhong	891	75.60	4838.40	1627.9	6301.15
Changzhi	990	97.34	6229.44	1584.1	7894.44
Linfen	783	2.84	181.44	1580.45	229.41
Jincheng	504	52.92	3386.88	1525.7	4133.89
Yuncheng	1152	0	0	1500.15	0
Summary	6453	677.57	43,364.16	—	56,177.68

The most suitable area for centralized photovoltaic installed capacity and annual power generation in each city is shown in Table 7. The most suitable area for centralized photovoltaic development in the province is 13,941 km², accounting for 8.90% of the total area of the province. The total installed capacity of photovoltaic modules reaches 627,345 MW, and the annual power generation is 821.2×10^3 GWh. In terms of specific cities, the most suitable area in Xinzhou is the largest compared with other cities of the Shanxi province. The total installed capacity of Xinzhou is 213,435 MW, and the annual power generation is 277.3×10^3 GWh.

Table 7. Statistics of centralized photovoltaic installed capacity and annual power generation potential in suitable areas of Shanxi province.

City Name	The Area of the Most Suitable Area (km ²)	Total Installed Capacity (MW)	Annual Power Generation (GWh)
Datong	3060	137,700	183,350.30
Shuozhou	1602	72,090	95,568.27
Xinzhou	4743	213,435	277,337.45
Lvliang	1134	51,030	66,457.39
Taiyuan	945	42,525	55,381.16
Yangquan	1026	46,170	59,454.03
Jinzhong	1377	61,965	80,698.26
Changzhi	9	405	513.25
Linfen	0	0	0
Jincheng	0	0	0
Yuncheng	45	2025	2430.24
Summary	13,941	627,345	821,190.35

As presented in Table 8, in 2021, the total social power consumption of Shanxi Province is 260.79×10^3 GWh. The annual power generation potential of distributed photovoltaic is 56.2×10^3 GWh, which is 21.54% of the total social power consumption of the province. The annual power generation potential of centralized photovoltaic is 821.2×10^3 GWh, which is 3.15 times the total social power consumption of the province. In summary, Shanxi province is rich in solar energy resources and has great potential for photovoltaic power development and utilization, especially in the northern regions including Datong, Shuozhou and Xinzhou. Under the background of transformation and upgrading of fossil energy, it is very important for Shanxi to develop solar energy based on the national

positioning of the power export base and to make a contribution to the achievement of the “peak carbon dioxide emissions and carbon neutrality”.

Table 8. Photovoltaic power generation potential statistics of cities in Shanxi Province.

City Name	Annual Growth Potential of Distributed pv (GWh)	Annual Growth Potential of Concentrated pv (GWh)	Total (GWh)	Electricity Consumption of the Whole Society in 2021 (GWh)
Datong	6603.49	183,350.3	189,953.79	18,600
Shuozhou	5933.11	95,568.27	101,501.38	14,130
Xinzhou	7623.01	277,337.45	284,960.46	15,220
Lvliang	8900.37	66,457.39	75,357.76	28,470
Taiyuan	6222.38	55,381.16	61,603.54	28,853
Yangquan	2336.44	59,454.03	61,790.47	9010
Jinzhong	6301.15	80,698.26	86,999.41	25,079
Changzhi	7894.44	513.25	8407.69	36,186
Linfen	229.41	0	229.41	24,750
Jincheng	4133.89	0	4133.89	22,780
Yuncheng	0	2430.24	2430.24	33,770
Summary	56,177.68	821,190.35	877,368.04	260,790

4. Conclusions

In this study, a hybrid GIS multi-dimensional evaluation method has been developed for solar energy potential in the raster grid scale. The raster grid scale is used as the minimum research scale, which could not only deal with the distributed photovoltaic potential but could also calculate the centralized photovoltaic potential. The main research results are as follows:

(1) The average annual total horizontal solar radiation in Shanxi province is 4770–5500 MJ/m² and gradually decreases from north to south. The total horizontal solar radiation in the central basin is smaller than that in the two sides of the same latitude, and the high value area appears in the northern part of Shanxi province. The seasonal fluctuation range of the total horizontal solar radiation is 160~300 MJ/m², and the radiation in summer is the largest among four seasons.

(2) From 1987 to 2016, the total horizontal solar radiation and annual sunshine hours decreased at rates of 74.9 MJ/(m²·10a) and 88.8 h/10a, respectively, with a significant decreasing trend ($p < 0.01$). Based on the regional statistical results, Taiyuan has the smallest decline in total horizontal solar radiation, and Jincheng has the smallest decline in annual sunshine hours, while Yangquan has the largest decrease in total horizontal solar radiation and annual sunshine hours in 30 years, which are 102.5 MJ/(m²·10a) and 126.4 h/10a, respectively.

(3) The total area suitable for distributed photovoltaic development in Shanxi province is 6453 km²; the area for installing photovoltaic modules is 677.6 km²; the installed capacity of photovoltaic modules is 43,364.16 MW; and the annual power generation potential reaches 56.2×10^3 GWh. The most suitable area for centralized photovoltaic development in the province is 13,941 km²; total installed capacity of photovoltaic modules reaches 627,345 MW; and the annual power generation is 821.2×10^3 GWh.

The results indicate that the developed method could effectively deal with problems associated with the solar energy potential and the suitable area in the raster grid scale. However, there is still some uncertainty, and further research work needs to be done. For example, data acquisition has certain limitations due to the large number of required data types and long time limit. Thirty years of radiation data is usually appropriate for the assessment of regional solar energy resources, and at least ten years of data should be collected if the requirements are not met. In terms of suitable development of photovoltaic, more refined topography and land use type data will also greatly improve the research

results. In addition, in terms of suitable development and utilization of photovoltaic power stations, more detailed terrain and land use type data will also greatly improve and enhance the research results.

Author Contributions: Conceptualization, L.C. and Y.S.; methodology; validation, Y.S.; investigation, S.L.; writing—original draft preparation, L.C.; writing—review and editing, J.Z. All authors have read and agreed to the published version of the manuscript.

Funding: This research was funded by National Natural Science Foundation of China, grant number 41901251.

Data Availability Statement: Not applicable.

Conflicts of Interest: The authors declare no conflict of interest.

References

- Zhou, Z.; Lin, A.; He, L.; Wang, L. Evaluation of Various Tree-Based Ensemble Models for Estimating Solar Energy Resource Potential in Different Climatic Zones of China. *Energies* **2022**, *15*, 3463. [\[CrossRef\]](#)
- Shahsavari, A.; Akbari, M. Potential of solar energy in developing countries for reducing energy-related emissions. *Renew. Sustain. Energy Rev.* **2018**, *90*, 275–291. [\[CrossRef\]](#)
- Yakubu, R.O.; Ankoh, M.T.; Mensah, L.D.; Quansah, D.A.; Adaramola, M.S. Predicting the Potential Energy Yield of Bifacial Solar PV Systems in Low-Latitude Region. *Energies* **2022**, *15*, 8510. [\[CrossRef\]](#)
- Hammer, A.; Heinemann, D.; Hoyer, C.; Kuhlemann, R.; Lorenz, E.; Müller, R.; Beyer, H.G. Solar energy assessment using remote sensing technologies. *Remote Sens. Environ. Interdiscip. J.* **2003**, *86*, 423–432. [\[CrossRef\]](#)
- Mahmud, A.M.; Kahsay, M.B.; Hailesilasie, A.; Hagos, F.Y.; Gebray, P.; Kelele, H.K.; Gebrehiwot, K.; Bauer, H.; Deckers, S.; De Baerdemaeker, J.; et al. Solar Energy Resource Assessment of the Geba Catchment, Northern Ethiopia. *Energy Procedia* **2014**, *57*, 1266–1274. [\[CrossRef\]](#)
- Escobar, R.A.; Cortés, C.; Pino, A.; Pereira, E.B.; Martins, F.R.; Cardemil, J.M. Solar energy resource assessment in Chile: Satellite estimation and ground station measurements. *Renew. Energy* **2014**, *71*, 324–332. [\[CrossRef\]](#)
- Xu, S.; Jiang, H.; Xiong, F.; Zhang, C.; Xie, M.; Li, Z. Evaluation for block-scale solar energy potential of industrial block and optimization of application strategies: A case study of Wuhan, China. *Sustain. Cities Soc.* **2021**, *72*, 103000. [\[CrossRef\]](#)
- Rylatt, M.; Gadsden, S.; Lomas, K. GIS-based decision support for solar energy planning in urban environments. *Comput. Environ. Urban Syst.* **2001**, *25*, 579–603. [\[CrossRef\]](#)
- Groppi, D.; de Santoli, L.; Cumo, F.; Garcia, D.A. A GIS-based model to assess buildings energy consumption and usable solar energy potential in urban areas. *Sustain. Cities Soc.* **2018**, *40*, 546–558. [\[CrossRef\]](#)
- Firozjaei, M.K.; Nematollahi, O.; Mijani, N.; Shorabeh, S.N.; Firozjaei, H.K.; Toomanian, A. An integrated GIS-based Ordered Weighted Averaging analysis for solar energy evaluation in Iran: Current conditions and future planning. *Renew. Energy* **2019**, *136*, 1130–1146. [\[CrossRef\]](#)
- Cheng, L.; Zhang, F.; Li, S.; Mao, J.; Xu, H.; Ju, W.; Liu, X.; Wu, J.; Min, K.; Zhang, X.; et al. Solar energy potential of urban buildings in 10 cities of China. *Energy* **2020**, *196*, 117038.1–117038.16. [\[CrossRef\]](#)
- Diner, F. The analysis on photovoltaic electricity generation status, potential and policies of the leading countries in solar energy. *Renew. Sustain. Energy Rev.* **2011**, *15*, 713–720. [\[CrossRef\]](#)
- Girard, A.; Gago, E.J.; Ordoñez, J.; Muneer, T. Spain's energy outlook: A review of PV potential and energy export. *Renew. Energy* **2016**, *86*, 703–715. [\[CrossRef\]](#)
- Rosenbloom, D.; Meadowcroft, J. Harnessing the Sun_ Reviewing the potential of solar photovoltaics in Canada. *Renew. Sustain. Energy Rev.* **2014**, *40*, 488–496. [\[CrossRef\]](#)
- Urban, F.; Geall, S.; Wang, Y. Solar PV and solar water heaters in China Different pathways to low carbon energy. *Renew. Sustain. Energy Rev.* **2016**, *64*, 531–542. [\[CrossRef\]](#)
- Vardimon, R. Assessment of the potential for distributed photovoltaic electricity production in Israel. *Renew. Energy* **2011**, *36*, 591–594. [\[CrossRef\]](#)
- Fillol, E.; Albarelo, T.; Primerose, A.; Wald, L.; Linguet, L. Spatiotemporal indicators of solar energy potential in the Guiana Shield using GOES images. *Renew. Energy* **2017**, *111*, 11–25. [\[CrossRef\]](#)
- Huang, T.; Wang, S.; Yang, Q.; Li, J. A GIS-based assessment of large-scale PV potential in China. *Energy Procedia* **2018**, *152*, 1079–1084. [\[CrossRef\]](#)
- Lau KK, L.; Lindberg, F.; Johansson, E.; Rasmussen, M.I.; Thorsson, S. Investigating solar energy potential in tropical urban environment: A case study of Dar es Salaam, Tanzania. *Sustain. Cities Soc.* **2017**, *30*, 118–127.
- Polo, J.; Bernardos, A.; Navarro, A.; Fernandez-Peruchena, C.; Ramírez, L.; Guisado, M.V.; Martínez, S. Solar resources and power potential mapping in Vietnam using satellite-derived and GIS-based information. *Energy Convers. Manag.* **2015**, *98*, 348–358. [\[CrossRef\]](#)

21. Li, C.; Shi, H.; Cao, Y.; Wang, J.; Kuang, Y.; Tan, Y.; Wei, J. Comprehensive review of renewable energy curtailment and avoidance: A specific example in China. *Renew. Sustain. Energy Rev.* **2015**, *41*, 1067–1079. [[CrossRef](#)]
22. Zhang, Y.; Ren, J.; Pu, Y.; Wang, P. Solar energy potential assessment: A framework to integrate geographic, technological, and economic indices for a potential analysis. *Renew. Energy* **2020**, *149*, 577–586. [[CrossRef](#)]
23. Tang, Y.; Feng, F.; Guo, Z.; Feng, W.; Li, Z.; Wang, J.; Sun, Q.; Ma, H.; Li, Y. Integrating principal component analysis with statistically-based models for analysis of causal factors and landslide susceptibility mapping: A comparative study from the Loess Plateau area in Shanxi (China). *J. Clean. Prod.* **2020**, *277*, 124–159. [[CrossRef](#)]
24. Niu, Z.; Xiong, J.; Ding, X.; Wu, Y. Analysis of China's Carbon Peak Achievement in 2025. *Energies* **2022**, *15*, 5041. [[CrossRef](#)]
25. SSY. *Shanxi Statistical Yearbook*; Shanxi Statistical Publishing House: Taiyuan, China, 2021.
26. NBS. *Statistical Bulletin for National Economic and Social Development*; The People's Government of Shanxi Province: Taiyuan, China, 2021.
27. Elagib, N.; Mansell, M.G. New approaches for estimating global solar radiation across Sudan. *Energy Convers. Manag.* **2000**, *41*, 419–434. [[CrossRef](#)]
28. Duffie, J.A.; Beckman, W.A. *Solar Engineering of Thermal Processes*, 3rd ed.; John Wiley & Son: New York, NY, USA, 2006.
29. Oliver, M.A.; Webster, R. Kriging: A method of interpolation for geographical information systems. *Int. J. Geogr. Inf. Syst.* **1990**, *4*, 313–332. [[CrossRef](#)]
30. IEC 61724:1998; Photovoltaic System Performance Monitoring—Guidelines for Measurement, Data Exchange and Analysis. International Electrotechnical Commission: Geneva, Switzerland, 1998; German Version EN 61724:1998. p. 61724.
31. Liu, G.X.; Wu, W.X.; Zhang, X.J.; Zhou, Y. Study for evaluating roof-mounted available solar energy resource—Case in jiangsu province according to its 2000data. *Resour. Environ. Yangtze Basin* **2010**, *19*, 1242–1248.

Disclaimer/Publisher's Note: The statements, opinions and data contained in all publications are solely those of the individual author(s) and contributor(s) and not of MDPI and/or the editor(s). MDPI and/or the editor(s) disclaim responsibility for any injury to people or property resulting from any ideas, methods, instructions or products referred to in the content.